



Cite this: DOI: 10.1039/c6pp00196c

Ag(Ag₂O)–ZrO₂–Y₂O₃ photosensitive composites: influence of synthesized routes on structure and properties

O. Gorban,* I. Danilenko, S. Gorban, G. Volkova, V. Glazunova and T. Konstantinova

It was shown that Ag(or Ag₂O)–ZrO₂–Y₂O₃ formation occurs due to the complex process of decomposition and structure transformation of oxide materials and Ag-complexes. Differences in the decomposition temperatures of Ag-complexes, in particular, and their melting temperatures, and the transformation of ZrO₂–Y₂O₃ NPs morphology leads to the creation of composite structure of two types: an Ag–NPs/zirconia matrix and zirconia core/Ag-shell. It was shown that for these composites the temperature is an effective approach for controlling the NPs sizes for both components (Ag clusters and zirconia NPs), the defectiveness of the complex oxide and their optical properties, in particular the photosensitive to visible irradiation range.

Received 11th June 2016,
Accepted 6th October 2016

DOI: 10.1039/c6pp00196c

www.rsc.org/pps

1. Introduction

Heterogeneous systems designers have a tendency to use complex composite structures where special properties of the interfaces are important.¹ The creation of metal/oxide composite materials may significantly enhance basic oxide materials' functionality, in particular the optical, electrochemical, conductivity and photosensitivity,² due to the possibility of reversible electron transfer between components of the composite at excitation of those materials in different irradiation ranges. Ag or silver dioxide (Ag₂O)-modified zirconia are promising composite structures for chemistry, environmental media, medicine, the electronics industry and other fields.³

Silver (Ag), gold (Au) and platinum (Pt) are often used as metal components for surface decoration of wide band gap semiconductor materials, such as titanium dioxide (TiO₂), zinc oxide (ZnO) and zirconium dioxide (ZrO₂). In practice, composite materials containing Ag NPs and oxide (NPs or matrix) are created by a variety of methods; for example low-energy ion beam deposition, sol-gel, direct metal implanting, light ion irradiation of an ion exchange oxide matrix, evaporation-condensation, using a very exotic leaf extract assisted bioreduction process, and other methods.^{4–7}

Usually, mono- or polycrystalline oxide particles and films are used as substrates (or matrix) for the implantation of metals to the oxides for the creation of composite materials.^{4,5,7,8} The usage of energy in the technology of creating metal/oxide can

lead to significant changing in the surface state and lattice of the modified oxide. Thus, the authors⁹ showed that irradiation of cubic zirconia monocrystal by noble metal ions led to incorporation of ions into crystals with a penetration thickness up to 1.5 μm and to form a complex of noble metal with Zr ions of the crystal lattice. These complexes were destroyed with subsequent heat-treatment of the composite material.

For zirconia, which has some polymorphs (monoclinic, tetragonal or cubic), the development of technologies to create noble metal/oxide without high-energy actions on the oxide component is a difficult task. Wet chemistry methods are cheaper variants for the synthesis of noble/metal composite and allow the controlling of structures and properties of the composite by changing the electronic state of Ag in the oxide matrix or oxide polymorph by varying the synthesis conditions, in particular, temperature or reduction type.^{7,8,10–17} Thus, the oxygen vacancies in a tetragonal zirconia crystal leads to the formation of a surface state in which Ag ions are included in the complex with neighbouring oxygen vacancies and the dispersion of Ag is higher in this phase than it is in the monoclinic phase.¹¹ The changing of zirconia matrix to alumina, to obtain Ag metal nanoparticles (NPs) in an oxide is practically impossible because the Ag ions build in the crystal lattice and form aluminium-oxygen-silver (Al–O–Ag) bonds up to 900 °C.¹⁷ In contrast, when creating a silver-germanium dioxide (Ag–GeO₂) composite structure, the temperature is a factor for controlling the size of the Ag NPs, and therefore the use of a low temperature range (150 °C–350 °C) leads to the formation of Ag NPs with a wide size distribution (the size of the Ag NPs changes from 5 nm to 50 nm as the temperature changes from 150 °C to 350 °C).¹⁸ The authors⁷ also showed

Materials science department, Donetsk institute for physics and engineering NAS of Ukraine, Kyiv, Nauki av. 46, 03680 Ukraine. E-mail: oxanagt@ukr.net

that the calcination of sol-gel films Ag/ZrO₂ in the low temperature range of 200 °C–300 °C leads to the formation of two set sizes of Ag⁰ NPs in the amorphous zirconia films, which are 20 and 80 nm; plasmonic resonance in these systems was observed at wavelengths about 450 and 500 nm, respectively. Investigation of the influence of the amount of Ag on the structure and optical properties of Ag:ZrO₂ thin films, which were formed at 300 °C, showed the dependence of Ag NPs size on the silver quantity. It was shown that the increasing of Ag loading in zirconia matrix led to the growth of the Ag NPs size from 7 to 20 nm and estimated wavelengths for two extreme values were 470 nm and 520 nm.⁸ The optical spectra of Ag NPs in sol-gel films that were formed at a higher temperature range of 500 °C–600 °C showed the presence of two peaks at 470 and 520 nm with an intensity dependence on the temperature used.¹² The plasma frequency, which was estimated for zirconia materials, corresponds to 452 nm.⁴ Such optical properties of Ag/zirconia strongly depended on the synthesis history and evolution of Ag NPs with heat-treatment, which is described as a set of sequential processes, such as the interaction of Ag NPs with an oxide matrix, the destruction of a complex oxide and the formation of Ag NPs with a narrower size distribution on the oxide surface.¹⁴ X-ray photoelectron spectroscopy (XPS) investigation showed that, for Ag-modified zirconia, temperature may be used to create an Ag shell/zirconia core type composite.¹² At the same time, under photo-reduction conditions, different electronic states of Ag in the composite can be observed. The XPS shows the presence of silver(I) oxide (Ag₂O) (Ag 3d_{5/2} = 367.7 eV), Ag (368.4 eV) and a transition charge state (368.8 eV),^{12,13} and for another case, electron spin resonance (ESR)^{15,16} has been shown to exist in the creation of Ag⁺–Ag⁰ clusters in bulk or on the surface of the oxide particles. In other words, the type of oxide matrix, the temperature of the treatment and the reduction conditions may be important factors for controlling the composite morphology, charge state and dispersity of Ag NPs and their properties.

At the same time, temperature is also a factor for controlling the size, morphology, surface state and fractal dimension of the NPs in a zirconia matrix, as well as the degree of connection that the NPs have with each other.^{19,20} Zirconia is formed from amorphous zirconium hydroxide as a result of the sequential processes of dehydration (up to 300 °C), crystallization (400 °C–500 °C), destruction of the amorphous matrix (400 °C–500 °C) and dispersion of the zirconia NPs (above the crystallization temperature). It is also known that different zirconia salts have different melting and decomposition temperatures, so argentum nitrate has a lower melting temperature (209 °C) and decomposition (near 350 °C) than argentum chloride (melting near 450 °C). We can see that the Ag complexes that are built using different ligands (nitrate (NO₃[–]) and chlorine (Cl[–]) ions) will also have different melting and decomposition temperatures. This provides the possibility to create a composite structure based on zirconia with Ag₂O or metallic Ag NPs, which are built upon new synthesis principles. In this approach, silver complexes with different structures are used as precursors. Silver complex ligands can

consist of ammonium groups, hydroxyl groups, water or other inorganic ions. One of the features of the realised synthesis is the simultaneous formation of complex oxide and silver complexes as a common system in a co-precipitation process, and in its subsequent thermal treatment. This study presents different routes that can be used to prepare a composite structure based on zirconia that allow variations not only in the morphology of the system and the size of the particles or clusters of the separate components of the composites, but also their photosensitive activity. Thus, when creating these types of composite structures questions arise about the structure of the oxide component, the electronic state of the metal, the changes based on variations in temperature or the reduction treatments and the interrelationship between their characteristics and the photosensitive properties of the composites.

2. Experimental

ZrO₂–Y₂O₃–Ag₂O composites were synthesized with a co-precipitation technique using ZrOCl₂·*n*H₂O or (ZrO(NO₃)₂), Y(NO₃)₃ and AgNO₃ salts. The amount of zirconium salt was 0.87 M. The amount of Y(NO₃)₃ was used in a quantity that was equal to 3 mol% as calculated for Y₂O₃ compared to ZrO₂. The amount of AgNO₃ was used in a quantity that was equal to 1 mol% as calculated for Ag₂O compared to ZrO₂. All used chemicals were of chemical grade purity. The water solutions of salts were mixed together on a propeller and stirred for 30 min. The precipitated gel was obtained by adding an aqueous solution of ZrOCl₂·*n*H₂O or (ZrO(NO₃)₂), Y(NO₃)₃ and AgNO₃ in NH₄OH aqueous water solution with continuous stirring. The pH value was 8. The gelation was continued for one hour at room temperature. After that the precipitate was recovered by filtration with a vacuum pump. The gel was washed by distilled water at pH 6. After washing and filtration, the hydrogel was dried in a microwave furnace with a 700 W output power and at a 2.45 GHz frequency. The dried hydroxides were calcined in a resistive furnace at different temperatures with a 2 h dwelling time. For the reduction of Ag in the Ag₂O–ZrO₂–Y₂O₃ composite structure, the following procedures were used:

- a suspension was of Ag₂O–ZrO₂–Y₂O₃ powders was prepared in a 1 : 3 ratio at pH 8;
- a reducing agent solution of 0.04 M glucose was prepared;
- the suspension and glucose solution were mixed with each other;
- the Ag NPs were reduced with 700 W under MW irradiation for 10 minutes, and then the suspension was filtered;
- the Ag–ZrO₂–Y₂O₃ composite was dried in a furnace at 140 °C.

The powders were characterized by XRD (Dron-3) with Cu-Kα radiation for crystallite sizes and quantitative phase analyses. Particle sizes of different calcined powders were estimated by means of transmission electron microscopy (JEM 200, Jeol, Japan). The photosensitive properties of Ag₂O–ZrO₂–Y₂O₃– nano-powders were measured on a Cary 5000 UV-Vis-NIR spectrometer (Agilent Technologies, USA). The ESR investigation was carried out with an ESR spectrometer CMS-8400 (Adani, Belarus).

3. Results and discussion

The choice of the oxide matrix (ZrO_2 -3 mol% Y_2O_3) was determined by the possibility of creating a tetragonal phase with oxygen vacancies that allows the formation of smaller silver clusters on the surface or in the matrix of the tetragonal zirconia in comparison to other polymorphic forms.¹¹ As noted above, the type of synthesis method used enables one to obtain the oxide materials as amorphous or crystalline nanoparticles (NPs) with different sizes and surface states, as a result of the set of processes that are applied. The scheme used for the formation of the oxide matrix at different heat-treatments is presented in Fig. 1.

In the process of drying under microwave (MW) irradiation, the amorphous zirconium hydroxide hydrogel ($\text{Zr}(\text{Y})\text{O}(\text{OH})_{2-n}\text{H}_2\text{O}$) lost water that was condensed in the porous hydrogel (up to 70%). According to the differential scanning calorimetry (DSC) data, the heating of amorphous zirconia ($\text{ZrO}_2\text{-Y}_2\text{O}_3\cdot(n-x)\text{H}_2\text{O}$) allowed the future loss of the physically- and chemically-adsorbed water; the water was removed more quickly when the temperature range was 50 °C–300 °C (up to 29 wt%), and water was removed more slowly when the temperature was increased to 700 °C (the water quantity was 46 wt%). In the temperature range of 400 °C–500 °C, the amorphous zirconia crystallites ($\text{ZrO}_2\text{-Y}_2\text{O}_3$) were formed. The transfer to isothermal regimes led to an increase in the size of the oxide matrix NPs with increasing calcination temperature.¹⁹ As can be seen, amorphous zirconium hydroxide was formed by the amorphous zirconia NPs connected to each other, and the structure could be described as porous. The crystalline zirconia NPs were formed at temperatures above the crystallization temperature, and the system could be described as dispersive. Thus, the zirconia matrix had a different morphology, and it showed the transfer from a porous structure to a dispersive system with different NPs sizes and degree of connection depending on the calcination temperature.^{20,21}

A. Features of the formation of the composite structure in amorphous zirconia matrix

One features of the determined $\text{Ag}_2\text{O-ZrO}_2\text{-Y}_2\text{O}_3$ synthesis is the simultaneous formation of complex oxide and silver complexes as a common system in the co-precipitation process and its subsequent thermal treatment.

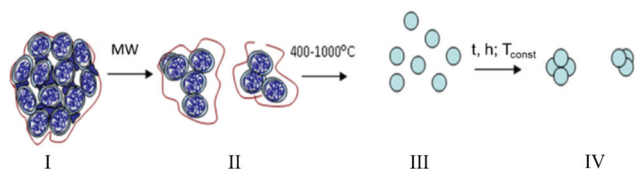


Fig. 1 Scheme of transform ZrO_2 -3 mol% Y_2O_3 under different treatment. I – Amorphous zirconium hydroxide hydrogel (it are dried under mw irradiation); II – amorphous zirconia (it is heating in non-isothermal regims in region 400–1000 °C); III – crystalline oxide (it is heating at T_{const} in region 400–1000 °C due to 2 hour).

In this approach, silver complexes were used as precursors in contrast to the traditional scheme of preparing catalysts. Ligands can be ammonium groups, hydroxyl groups, water or other inorganic ions. Differences in the silver complex structure led to variation in the decomposition temperature. Two processes, the zirconia matrix formation and silver complex decomposition or melting occurred simultaneously. This allowed for variations not only in the morphology of the system, but also in the sizes of the particles or clusters of the separate components of the composites.

Fourier transform infrared spectroscopy (FTIR) of the synthesized amorphous systems showed a set of absorption bands (3167 cm^{-1} and 3050 cm^{-1}) and narrow bands with frequencies at 763 cm^{-1} and 826 cm^{-1} (Fig. 2), demonstrating the formation of ammonium complexes of silver $[\text{Ag}(\text{NH}_3)_{2-m}(\text{H}_2\text{O})_m]\text{X}$, where X is either the chloride (Cl^-) or nitrate (NO_3^-) ion depending on the type of zirconium salt that is used in the synthesis (Fig. 2). The presence of bands at 487 cm^{-1} and 647 cm^{-1} is assigned to the zirconium–oxygen–zirconium (Zr-O-Zr) bonds that are oriented in the tetragonal phase. In the ESR spectra, the signal from Ag^0 is absent for such systems.

It is known that the structure of amorphous zirconia is porous regardless of the type of zirconium salt that is used in the synthesis^{16,17} because the reduction of silver may be occurring in the pores. The ESR data for $\text{Ag-ZrO}_2\text{-Y}_2\text{O}_3$ confirm our proposition (Fig. 3).

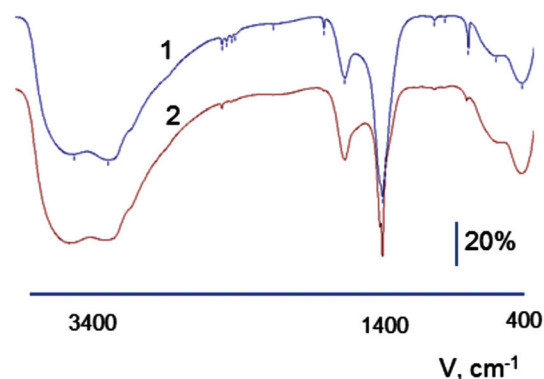


Fig. 2 FTIR spectra of $\text{Ag}_2\text{O-ZrO}_2\text{-Y}_2\text{O}_3$ amorphous composite which was synthesized based on salts (1) nitrate, (2) chloride.

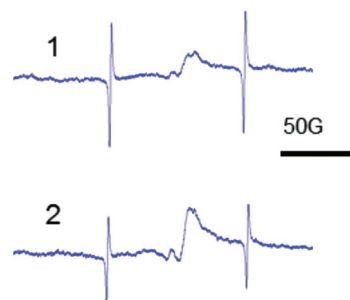


Fig. 3 ESR spectra of amorphous $\text{Ag-ZrO}_2\text{-Y}_2\text{O}_3$ which synthesized from zirconium salt: (1) nitrate, (2) chloride.

The isotropic signal with $g_{\text{iso}} = 2.003$ in the ESR spectra corresponds to the formation of Ag^0 NPs.²² The ESR data provides evidence of the formation of $\text{Ag}/\text{ZrO}_2\text{-Y}_2\text{O}_3$ composites, which has the structure of Ag NPs in the porous $\text{ZrO}_2\text{-Y}_2\text{O}_3$ matrix (Fig. 3). It should be noted that the isotropic signal corresponding to Ag^0 NPs in the ESR spectra of the non-reduced $\text{Ag}_2\text{O-ZrO}_2\text{-Y}_2\text{O}_3$ amorphous systems was not observed.

B. Features of the formation of the composite structure in crystalline zirconia

B1. Forming of $\text{Ag}_2\text{O-ZrO}_2\text{-Y}_2\text{O}_3$ systems with different routes of preparation. According to the DSC data, in heat treatment of the synthesised amorphous $[\text{Ag}(\text{NH}_3)_{2-m}(\text{H}_2\text{O})_m]\text{X} + \text{ZrO}(\text{OH})_2\text{-Y}(\text{OH})_3$ ($\text{X} = \text{Cl}^-$ or NO_3^-) systems, the dehydration of zirconium hydroxide, decomposition of the silver complexes (or melting) and crystallization of the amorphous zirconia NPs were observed (Fig. 4).

Based on the DSC data, three processes, one endothermic and two exothermic, can be observed during the heating of the prepared amorphous systems. The endothermic process corresponds to dehydration, and it occurred at temperatures up to 200 °C. The maximum temperatures for these processes were practically equal (near 115 °C) for both systems, and the difference in the enthalpies of dehydration of these processes was near 1.8 kJ mol⁻¹. It is important to note that the dehydration parameters for the $\text{ZrO}_2\text{-Y}_2\text{O}_3$ and $\text{Ag}_2\text{O-ZrO}_2\text{-Y}_2\text{O}_3$ systems that were synthesised with nitrate and chloride zirconium salts were likely to change.

The first exothermal peak was observed at 253 °C and 263 °C for the systems that were synthesised from zirconium

chloride and nitrate, respectively. The process may correspond to the destruction or rebuilding of $[\text{Ag}(\text{NH}_3)_{2-m}(\text{H}_2\text{O})_m]\text{X}$ ($\text{X} = \text{Cl}^-$ or NO_3^-), in particular the removal of water, ammonium and the nitrate groups, and the formation of argentum oxide. Chloride ions were removed at higher temperatures (up to 900 °C). The enthalpies of these processes differed (105 J g⁻¹ when using chloride salts in contrast to 55 J g⁻¹ when using nitrate salts), and it may be connected to the difference in the stability of the Ag complex that occurs when using chloride and nitrate ligands.

Thermogravimetric (TG) investigations (TG data, see Fig. 4) show that the systems lost approximately an equal amount of water when heated up to 500 °C (30% and 34% when chloride and nitrate salts at synthesis, respectively). In the first step of dehydration up to 225 °C, the amount of water loss was 20% and 15% for chloride and nitrate, respectively. This is a feature of the formation of the oxide matrix, which was synthesised from the chloride salts. In the second stage (225 °C–280 °C), the amount of lost water was 6%–7%. The residual amount of water was lost when the temperature increased up to 700 °C.

The second exothermal peak corresponds to the crystallisation of the amorphous oxide matrix. The difference in the maxima of the crystallisation temperature was very small (about 5 °C), and the enthalpies for the crystallisation were practically equal (107 J g⁻¹ and 109 J g⁻¹ for nitrate and chloride, respectively). This provides evidence that the ordering in the formed crystal (defectiveness) was practically equal.

The XRD data confirmed these results and showed that all the $\text{Ag}_2\text{O-ZrO}_2\text{-Y}_2\text{O}_3$ crystals were tetragonal. However, silver oxide traces were found in the systems that were synthesised using chloride technology.

B2. Influence of the type of Ag complex on the composite structure. The ESR spectra of the reduced $\text{Ag-ZrO}_2\text{-Y}_2\text{O}_3$ systems that were synthesised with different precursors and calcined at 600 °C temperature are shown in Fig. 5. For the crystalline systems that were synthesised using nitrate technology, the ESR spectrum showed the presence of an isotropic signal with $g_{\text{iso}} = 2.003$ (similar to the amorphous systems) for Ag^0 and an anisotropic signal with $g_1 = 1.95$ and $g_2 = 1.98$ for

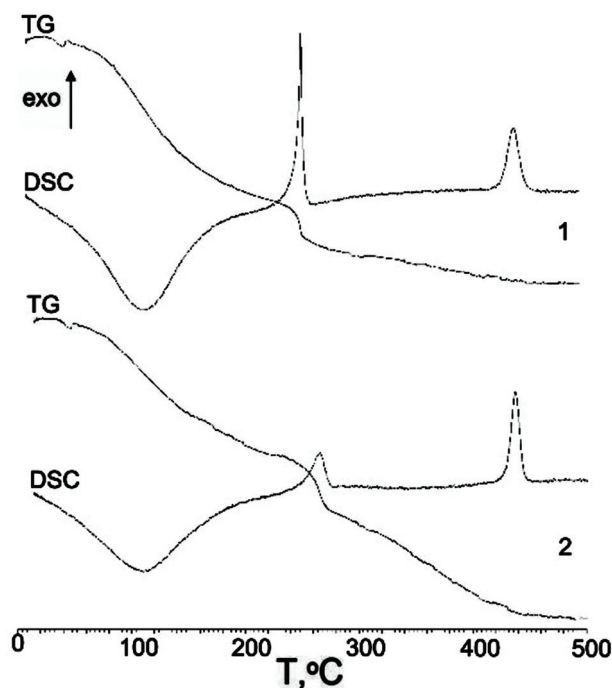


Fig. 4 DSC data of $\text{Ag}_2\text{O-ZrO}_2\text{-Y}_2\text{O}_3$ systems that are synthesized based on (1) chloride (2) nitrate salts.

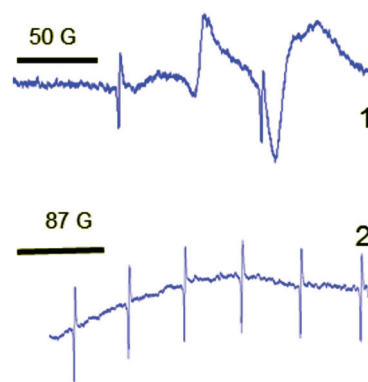


Fig. 5 ESR spectra of crystalline composite $\text{Ag-ZrO}_2\text{-Y}_2\text{O}_3$ that synthesized from zirconium salt (1) nitrate, (2) chloride.

Zr^{3+} . The last signal is assigned to the presence of Zr^{3+} centres. It was observed that the intensity of this signal decreased as the calcination temperature of the NPs was increased. This may show that the creation of composite materials with Ag NPs in zirconia matrix structures also occurs in amorphous systems.

For the Ag– ZrO_2 – Y_2O_3 case, which was obtained using chloride technology, the well-separated signal with $g_{\text{iso}} = 2.003$ for Ag^0 in the ESR spectra was not observed and the signal of Zr^{3+} was also absent. The ESR spectra results demonstrate a broad magnetic field signal range of 3150–3600 G. This signal may correspond to very small silver clusters, which are localised on the surface of the NPs. This may provide evidence of the formation of composite materials with a core/shell structure.

Transmission electron microscopy (TEM) investigations of the prepared reduced Ag– ZrO_2 – Y_2O_3 systems showed differences in the morphologies (Fig. 6), and confirmed that the proposed composite had an Ag^0 shell/ ZrO_2 – Y_2O_3 core when the composite was formed using the chloride route for the synthesis and an Ag^0 NPs in ZrO_2 – Y_2O_3 porous matrix when it is formed using the nitrate synthesis route. Detailed analysis of TEM data for the Ag– ZrO_2 – Y_2O_3 systems ($T_{\text{calc}} = 700^\circ\text{C}$ followed by reduction) (Fig. 6c) showed two sets of Ag^0 NPs present on the ZrO_2 – Y_2O_3 NPs surface, in particular, the sizes of the first type of Ag^0 NPs were about 1–1.5 nm and Ag^0 NPs of second type had a bigger size (about 4–5 nm). The first kind of Ag^0 NPs formed a shell of ZrO_2 – Y_2O_3 core and the large Ag^0 NPs had a decorated surface of composite.

B3. Influence of temperatures on the composite system properties. The optical properties of crystalline composite systems of Ag– ZrO_2 – Y_2O_3 and Ag_2O – ZrO_2 – Y_2O_3 that were synthesized using chloride technology showed a dependence on the calcination temperature and were influenced by the reduce atmosphere, see Fig. 7.

Analyses of these data in the Kubelka–Munka function ($F(R)$) showed that for composite systems, the red shift of edge of the fundamental absorption was observed in comparison with the ZrO_2 – Y_2O_3 system, see Fig. 7. The value of this shift for Ag_2O – ZrO_2 – Y_2O_3 and for Ag– ZrO_2 – Y_2O_3 depended on their calcination temperature.

Thus for the ZrO_2 – Y_2O_3 tetragonal crystal with size 18 nm ($T_{\text{calc}} = 700^\circ\text{C}$) the fundamental absorption edge value was 5.5 eV, but when transformed to the Ag_2O shell/ ZrO_2 – Y_2O_3 core systems, this values shifted to 5.2 and 4.7 eV for systems obtained at 700°C and 900°C calcination temperatures, respectively. The reduction of Ag in these systems did not change the edge of fundamental absorption values, see Fig. 7. In addition to the absorption of photons above the fundamental absorption edge of a complex oxide ZrO_2 – Y_2O_3 core (5.2 eV) in the spectrum of Ag_2O – ZrO_2 – Y_2O_3 (700°C), there is a fundamental absorption edge of Ag_2O (with a 3.9 eV energy). For the Ag_2O – ZrO_2 – Y_2O_3 (900°C) system in addition to absorption bands, which were mentioned above, the plasmonic absorption of photons with energies of 2.4 eV (515 nm) and 3.2 eV (384 nm) were observed. This is connected with the decomposition of Ag_2O near this temperature. Optical properties of composite NPs are due to the interaction of incident waves and electromagnetic oscillations, which are induced by dipoles. NPs may be described as dipoles because their sizes are less than the wavelength of an incident wave, and for estimation of their optical properties, the dipole quasi-static approach may be used. In this case, the quantitative characteristic is complex polarizability and for spherical NPs, polarizability may be estimated as follows:²³

$$\delta = 4\pi r^3 \frac{\epsilon_1 - \epsilon_0}{\epsilon_1 + 2\epsilon_0} \quad (1)$$

where ϵ_1 , ϵ_0 are the dielectric constant of zirconia and noble metal NPs and r is the NPs size. In case of the composite of the core/shell kind the polarizability is described as follows:

$$\delta = 4\pi r_s^3 \frac{\epsilon_s \epsilon_a - \epsilon_h \epsilon_b}{\epsilon_s \epsilon_a + 2\epsilon_h \epsilon_b} \quad (2)$$

where ϵ_h is the dielectric constant and

$$\epsilon_a = \epsilon_c(3 - 2P) + 2\epsilon_s P \quad (3)$$

$$\epsilon_b = \epsilon_c + \epsilon_s(3 - P) \quad (4)$$

$$P = 1 - \left(\frac{r_c}{r_s}\right)^3 \quad (5)$$

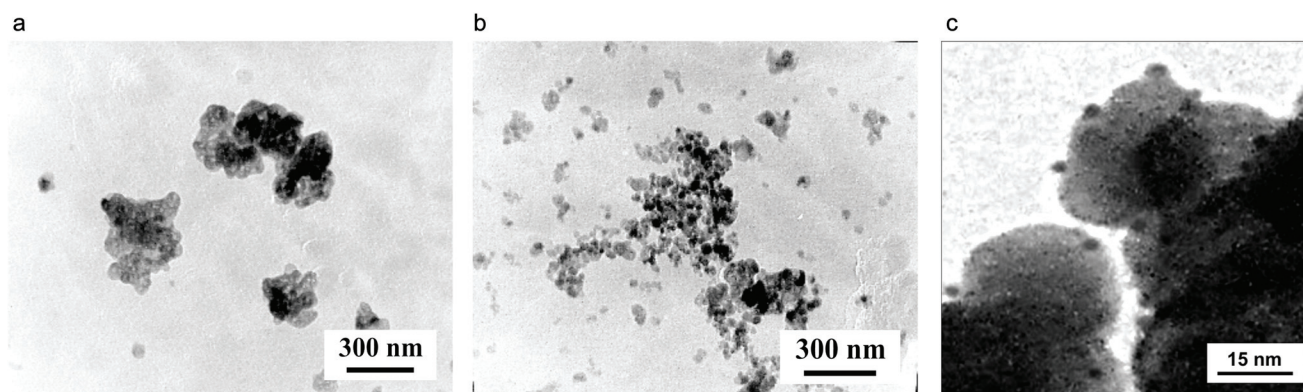


Fig. 6 Morphology of composite (TEM image) which was synthesized from zirconium salt (a) nitrate, (b) chloride, (c) magnification of section from (b).

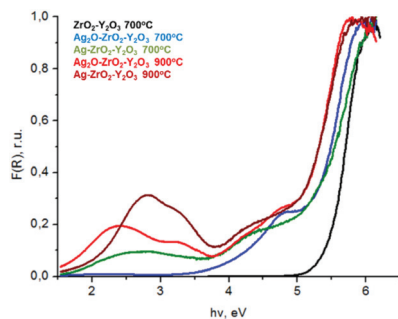


Fig. 7 UV-visible spectra of composite systems Ag(Ag₂O)-ZrO₂-Y₂O₃ which was synthesized by chloride technology with different regime of heat treatment.

when plasmon resonance is created, the increasing of the cross-section of absorption (σ_a) and scattering (σ_s) of metal NPs are observed. The cross-section of absorption (σ_a) and scattering (σ_s) in the dipole quasi-static approximation is related to its polarizability δ by the following expressions:

$$\sigma_a = k \text{Im}(\delta) \quad (6)$$

$$\sigma_s = \frac{k^4}{18\pi} |\delta|^2 \quad (7)$$

where k is the wave scalar.

Spherical NPs with sizes of 1–20 nm have one peak of plasmonic resonance if the interaction between NPs does not occur.

All our systems showed two peaks plasmon resonance (Fig. 7). The first peak near 3.2 eV may correspond to the Ag⁰ spherical NPs with 4–5 nm size, which decorated the composite surface (Fig. 6c). Similar (6–7) NPs sized up to 15 nm have plasmon resonance at the same wavelength. The appearance of second peaks at 2.4–2.8 eV may be due to the same reasons; the first creation of core/shell structure with a thin Ag shell on a ZrO₂-Y₂O₃ core and strong electromagnetic interaction between Ag NPs in shell were confirmed by ESR spectroscopy. The peak shift at 2.4 eV towards a lower wavelength after reduction of silver by glucose demonstrated an increasing shell density in such composites. For example, Fig. 8 shows a theoretical spectra of the cross-section scattering *versus* wavelength that are estimated by eqn (1)–(7) for the composite structure. The estimated average Ag NPs size was 4–5 nm and the thickness of the Ag shell was about 1.3–1.5 nm.

Reduction treatment of the Ag₂O-ZrO₂-Y₂O₃ composite structure led to the formation of Ag⁰ clusters on an oxide NPs surface that absorbed radiation with 2.8 eV (440 nm) and 3.2 eV (384 nm) energies in the UV-visible range. For all composite systems below the edge of fundamental adsorption, we observed a tail in the spectrum (range 4–5 eV). This possibility corresponds to both Ag₂O traces in the composites and surface defects of ZrO₂-Y₂O₃, which were created due to the solution of silver ions in zirconia.

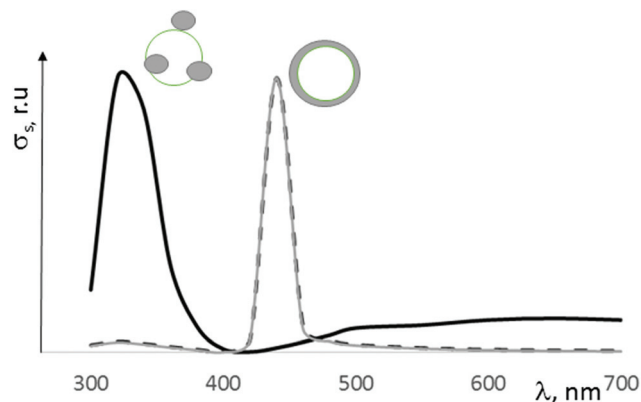


Fig. 8 Estimated cross-scattering values for different types of structures of Ag-ZrO₂-NPs with a calcination temperature of 900 °C.

4. Conclusion

The formation of Ag(or Ag₂O)-ZrO₂-Y₂O₃ occurs due to the complex process of decomposition and structure transformation of oxide materials and Ag-complexes. Differences in structure and stability of Ag-complexes, in particular their melting temperatures, and also dependence of oxide NPs morphology from calcination temperature allowed two types of composite structures to be realized: Ag(Ag₂O)-NPs/in zirconia matrix and Ag(Ag₂O)-shell zirconia core. It was shown that for these composites, temperature is an effective approach for controlling of NPs sizes of both components (Ag clusters and zirconia NPs), defectiveness of the composite and their optical properties, in particular the photosensitivity to visible irradiation range.

Acknowledgements

The authors are thankful for the H2020-MSCA-RISE-2015 Programme, the project N690968 NANOGUARD2AR and project N 47/15H of program NAS of Ukraine “Fundamental problems of creation of new nanomaterials and nanotechnologies” for financial support of their work.

Notes and references

- 1 Y. Ju-Nam and J. R. Lead, *Sci. Total Environ.*, 2008, **400**, 396.
- 2 *Nanocomposites and polymers with analytical methods*, ed. J. Cuppoletti, Rijeka, In Tech, 2011, p. 51.
- 3 D. Cui, F. Tian, S. R. Coyer, J. Wang, B. Pan, F. Gao, R. He and Y. Zhang, *J. Nanosci. Nanotechnol.*, 2007, **7**, 1639.
- 4 Y. Saito, Y. Imamura and A. Kitahara, *Nucl. Instrum. Methods Phys. Res., Sect. B*, 2003, **206**, 272.
- 5 T. Fujita, K. Ijima, N. Mitsui, K. Mochiduki and Y. Saito, *Jpn. J. Appl. Phys.*, 2007, **46**, 7362.

- 6 S. Vivekanandhan, M. Venkateswardlu, U. Rawls, M. Misra, A. Mohanty and N. Satyanarayana, *Ceram. Int.*, 2015, **41**, 3305.
- 7 E. Yokoyama, H. Sakata and M. Wakaki, *J. Mater. Res.*, 2009, **24**(8), 2541.
- 8 M. Kumar, P. K. Kulriya, J. C. Pivin and D. K. Avasthi, *J. Appl. Phys.*, 2011, **109**, 044311.
- 9 O. Gorshkov, M. Schenina, A. Kasatkin, D. Pavlov, I. Antonov, A. Bobrov and D. Filatov, *Letters in JTF*, 2015, **41**(11), 62.
- 10 Lj. Kundokovic and M. Flytrani-Stephanopoulos, *Appl. Catal., A*, 1999, **183**, 35.
- 11 R. Grabowski, J. Słoczyński, M. Śliwa, D. Mukha, R. P. Socha, M. Lachowska and J. Skrzypek, *ACS Catal.*, 2011, **1**(4), 266.
- 12 A. Eremenko, N. Smirnova, Iu. Gnatiuk, O. Linnik, N. Vityuk, Yu. Mukha and A. Korduban, *Chapter in Book 3: Composite Materials*, 2011, p. 2.
- 13 J. Matsuoka, R. Naruse, H. Nasu and K. Kamiya, *J. Non-Cryst. Solids*, 1997, **218**, 151.
- 14 F. Yang, X. Jing, J. Huang, D. Sun and Q. Li, *Ind. Eng. Chem. Res.*, 2015, **54**, 20.
- 15 M. Kumar and G. B. Reddy, *Plasmonics*, 2016, **11**(1), 261.
- 16 W. Gruenert, A. Brueckner, H. Hofmeister and P. Claus, *J. Phys. Chem. B*, 2004, **108**, 5709.
- 17 X. She and M. Flytzani-Stephanopoulos, *J. Catal.*, 2006, **237**, 79.
- 18 G. E. Malashkevich, G. P. Shevchenko, S. V. Serezhkina and P. P. Pershukovich, in *The 13th Int. Workshop on Sol-Gel Science and Technology*, University of California, Los Angeles, 2005, p. 415.
- 19 T. Konstantinova, I. Danilenko, V. Glazunova, G. Volkova and O. Gorban, *J. Nanopart. Res.*, 2011, **13**, 4015.
- 20 O. Gorban, S. Synyakina, G. Volkova, Y. Kulik and T. Konstantinova, *High Pressure Res.*, 2011, **32**(1), 72.
- 21 O. A. Gorban, S. A. Sinyakina, Yu. O. Kulik, T. A. Ryumshina, S. V. Gorban, I. A. Danilenko and T. E. Konstantinova, *Funct. Mater.*, 2010, **17**(4), 1.
- 22 A. D. Stevens and M. C. R. Symons, *Chem. Phys. Lett.*, 1984, **109**, 514.
- 23 V. Klimov, *Nanoplasmonics*, CRC Press Taylor and Francis group, Brooken, 2014, p. 593.